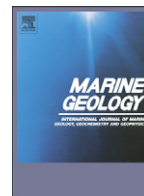




ELSEVIER

Contents lists available at ScienceDirect

Marine Geology

journal homepage: www.elsevier.com/locate/margeo

Shelf sedimentation on a tectonically active margin: A modern sediment budget for Poverty continental shelf, New Zealand

Andrea J. Miller, Steven A. Kuehl *

Virginia Institute of Marine Science, 1208 Greate Road, P.O. Box 1346, Gloucester Point, VA 23062, USA

ARTICLE INFO

Available online xxxx

Keywords:

Waipaoa River
continental margin
shelf sedimentation
 ^{210}Pb geochronology
 $^{239,240}\text{Pu}$ geochronology
sediment budget

ABSTRACT

The combination of high sediment yields and the prevalence of tectonically controlled accommodation on collision margins such as that adjacent to the Waipaoa River, NZ, create the potential for these areas to contain high-resolution records of natural and anthropogenic signals. This study describes modern (100-yr) sedimentation patterns off the Waipaoa and quantifies a sediment budget for the continental shelf, which is compared to long-term Holocene trends. ^{210}Pb and $^{239,240}\text{Pu}$ geochronologies reveal three main shelf depocenters. Two of these depocenters are located in subsiding synclinal basins on the mid-shelf, landward of the actively deforming Ariel and Lachlan anticlines. The depocenters exhibit accumulation rates ranging from 0.75 to 1.5 cm yr^{-1} and display both steady-state and non-steady-state ^{210}Pb activity profiles. Textural characteristics of the non-steady-state cores indicate the possible preservation of flood event layers. The third depocenter is located near the shelf break and has accumulation rates as high as 1.0 cm yr^{-1} . The inner shelf and central mid-shelf are characterized by low, uniform ^{210}Pb activity profiles and low accumulation rates, indicating that sediment is bypassing the inner shelf region and being deposited on the mid- to outer shelf. The modern sedimentation patterns seen in this study are similar to those for the Holocene, suggesting that regional tectonics are the major influence on Poverty shelf sedimentation. A modern, bulk sediment budget estimates that $3.6 \pm 0.9 \times 10^6 \text{ t yr}^{-1}$ of sediments remains on the shelf, amounting to only ~25% of the 15 Mt of sediments discharged from the river per year. This indicates massive export of sediments from the study area to the adjacent slope or along the shelf. In contrast, studies of the Mid-Late Holocene sediment budget in the same area indicate that the sediment input and shelf trapping have been roughly in balance. When compared with the modern budget, this suggests an extraordinarily rapid shift from shelf trapping to shelf bypassing, most likely driven by increasing sediment discharge in response to deforestation.

© 2009 Elsevier B.V. All rights reserved.

1. Introduction

Tectonically active continental margins are often characterized by small mountainous rivers carrying large sediment loads to narrow shelves (Milliman and Syvitski, 1992). In some cases, the tectonic activity on these shelves can result in deformation and the formation of mid-shelf synclinal basins, which can control sedimentation on both short and long timescales. For example, tectonically formed synclinal basins are the primary sediment repositories on the shelf for the Waipaoa and Waiapu Rivers in New Zealand, and the Eel River in California (Clarke, 1987; Foster and Carter, 1997; Lewis et al., 2004). Additionally, the large sediment input of these rivers has the potential to create a high-resolution stratigraphic record, which could enable both natural and anthropogenic perturbations to the system to be investigated. Alternatively, with the limited accommodation space on narrow shelves, much of the sediments delivered to collision margins

could be transported to the adjacent slopes and the deep sea even during high sea-level conditions (Milliman and Syvitski, 1992). Thus tectonically active margins may not follow the traditional sequence stratigraphy model, which predicts high-stand shelf trapping immediately following a rapid sea-level rise such as the Holocene Transgression; as shown in recent work on these settings (Alexander and Simoneau, 1999; Sommerfield and Nittrouer, 1999). Further analysis of active margin sedimentation patterns is needed in order to refine our understanding of sequence stratigraphy and stratigraphic signals of climate change and landscape evolution.

The Waipaoa River, located along the mountainous and tectonically active northeast region of the North Island, New Zealand (NZ), is one of the main focus sites for the MARGINS Source-to-Sink (S2S) program, which is sponsored by the National Science Foundation. An important objective of the S2S program is to determine how climate, tectonics, and anthropogenic impacts affect the processes responsible for the production, transport, and accumulation of sediments on margins (Gomez et al., 2001). Previous studies have suggested that the majority of the sediments leaving the Waipaoa River are deposited and preserved on the continental shelf due to the closed nature of the

* Corresponding author. Tel.: +1 804 684 7118.
E-mail address: kuehl@vims.edu (S.A. Kuehl).

shelf basin (Foster and Carter, 1997). However, recent results indicate that a portion of the sediments is being transported to the slope (Alexander et al., 2009–this issue). This suggests that both the continental shelf and slope presently are important final repositories for terrestrially derived sediments and can be informative records of natural and anthropogenic impacts. This study uses radioisotope geochronology to identify modern sedimentation patterns and provide a sediment budget for the shelf. A comparison between modern and Holocene sediment accumulation leads to a better understanding of the factors controlling sedimentation and provides insight into the impact of both natural and anthropogenic perturbations.

2. Regional setting

2.1. Tectonic and climate settings of the Waipaoa Catchment

The Waipaoa River is located on the East Coast of the North Island, NZ (Fig. 1) along the tectonically active Hikurangi Margin where the Pacific Plate is being obliquely subducted beneath the Australian Plate. At the Waipaoa mouth, freshwater and suspended sediments are delivered to Poverty Bay via the coastal plains of Gisborne. The catchment (2205 km²) originates in the axial mountain ranges where tectonic uplift is estimated at 4 mm yr⁻¹ with a maximum uplift of 10 mm yr⁻¹ (Berryman et al., 2000; Hicks et al., 2000). Geologic, climatic, and anthropogenic factors have resulted in high suspended-sediment concentration and sediment yield (Page et al., 2001). The Waipaoa River has the fourth highest suspended-sediment concentration of all NZ rivers with a mean of 1700 mg L⁻¹, and has an annual

sediment discharge of 15 Mt. (Griffiths, 1982; Hicks et al., 2000; Hicks et al., 2004).

The Waipaoa catchment is underlain by Cretaceous and Paleocene mudstone and argillite, Jurassic to Early Cretaceous greywacke, and Miocene–Pliocene sandstone, siltstone, and mudstone (Hicks et al., 2000; Page et al., 2001). These soft, fine-grained rocks are easily erodible and thus contribute much suspended-sediment to the Waipaoa River. Approximately 6750 m⁻² yr⁻¹ of sediments is eroded from the landscape; one of the world's highest sediment yields (Hicks et al., 2004). Contributing to this erosion is high precipitation, with an annual average rainfall of 1000 mm yr⁻¹ at the coast to greater than 2500 mm yr⁻¹ in the headwaters (Page et al., 2001; Wilmshurst et al., 1999). The sediments are mainly delivered to the river via gully erosion, earthflows, and shallow landsliding. Gully erosion dominates the erosional regime in the catchment; however, shallow landsliding frequently accompanies high rainfall events such as those associated with cyclones (Foster and Carter, 1997).

Modern land-use practices are another factor contributing to erosion in the catchment. Podocarp/hardwood forests were the indigenous vegetative cover of the Waipaoa catchment before Maori settlement occurred between 450 and 980 yr B.P. (Page et al., 2001; Wilmshurst, 1997). During this settlement, much of the podocarp forests were cleared by fires and replaced with a bracken fern-scrubland (Wilmshurst, 1997; Wilmshurst et al., 1997, 1999). This change in vegetation decreased the stability of the soil and led to a slight increase in soil erosion. A more dramatic increase in erosion occurred between 1880 and 1920 due to extensive deforestation by European settlers (Page et al., 2001; Wilmshurst, 1997; Wilmshurst et al., 1997, 1999).

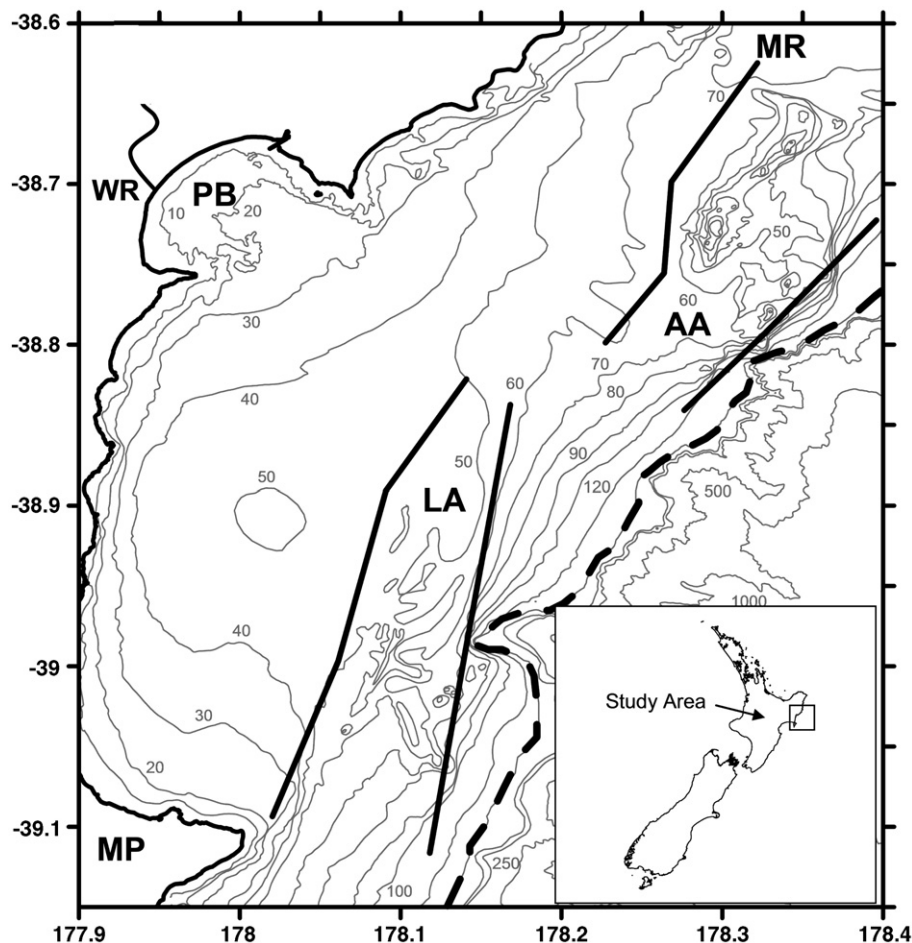


Fig. 1. Continental shelf off the Waipaoa River located on the North Island of New Zealand, with isobaths (m) provided by NIWA. WR = Waipaoa River, LA = Lachlan Anticline, AA = Ariel Anticline, PB = Poverty Bay, MR = Monowai Rocks, MP = Mahia Peninsula. Dashed line indicates shelf break located at 150 m. Solid lines outline the edges of the two mid-shelf anticlines.

The European settlers cleared the majority of the hardwood forests and fern-scrublands in the catchment and converted these lands to pastures. This greatly destabilized the soil which left it vulnerable to erosion and landsliding. Today, less than 3% of the indigenous forest-cover remains in the Waipaoa catchment.

2.2. Sedimentation on the Poverty Shelf

Much of the sediment carried by the Waipaoa River is transported to the adjacent continental shelf by hypopycnal plumes (Foster and Carter, 1997). These plumes carry sediments in a northeastward or southward direction on the shelf, depending upon prevailing wind-driven circulation. However, hyperpycnal plumes may be formed during intense floods that greatly increase the suspended-sediment concentration of the Waipaoa (Foster and Carter, 1997). Minimum suspended-sediment concentration in the Waipaoa River discharge would need to be between 37,100 and 40,300 mg L⁻¹ to generate a hyperpycnal plume off the river mouth; the recurrence interval for these plumes is estimated to be > 40 yr (Hicks et al., 2004).

The growing Ariel and Lachlan anticlines, located on the outer shelf (Fig. 1), are natural barriers that are thought to hinder sediments from dispersing to the slope (Foster and Carter, 1997). The shelf is also bordered by the Monowai Rocks to the north and the Mahia Peninsula located 65 km to the south. The shelf extends 22–26 km seaward to the shelf break at a water depth of 140–170 m (Foster and Carter, 1997). The circulation on the shelf is dominated by the semi-permanent East Cape Current, which travels along the shelf break (Carter et al., 1996; Foster and Carter, 1997). The East Cape Current has a net southward flow with periodic reversals resulting from

prolonged changes in wind direction (Carter et al., 2002). Circulation on the inner shelf is dominated by periodic incursions of the Wairarapa Coastal Current which flows to the north (Foster and Carter, 1997). The shelf circulation is only weakly affected by the tides.

Sediment facies on the continental shelf follow a pattern of fine sands on the inner shelf and silts and clays on the mid-shelf synclinal basins and the outer shelf (Foster and Carter, 1997; Wood, 2006). The transition from sand to mud occurs at approximately 30–40 m depth. The mud deposit extends from the middle shelf to the Ariel and Lachlan anticlines and through the corridor located between the anticlines to the continental slope (Foster and Carter, 1997). Gravel-sized sediments are located around rocky exposures associated with the Ariel and Lachlan anticlines (Foster and Carter, 1997).

3. Materials and methods

3.1. Field techniques and sampling

In January 2005, a suite of 85 kasten cores were collected aboard the *R/V Kilo Moana* on the continental shelf adjacent to the Waipaoa River for sedimentological and geochemical studies (Fig. 2). The majority of the sediment cores were collected between 26 to 75 m water depth on the shelf landward of the Ariel and Lachlan anticlines, with fewer cores collected between the seaward edge of the anticlines and the shelf break. Kastens cores are 3-m long gravity cores with a 12 × 12-cm cross-section. Onboard, sub-samples of all cores were collected for geochemical and textural analysis using a geometric sampling plan consisting of continuous 2-cm thick samples for the first 10 cm with successively larger intervals between samples as core

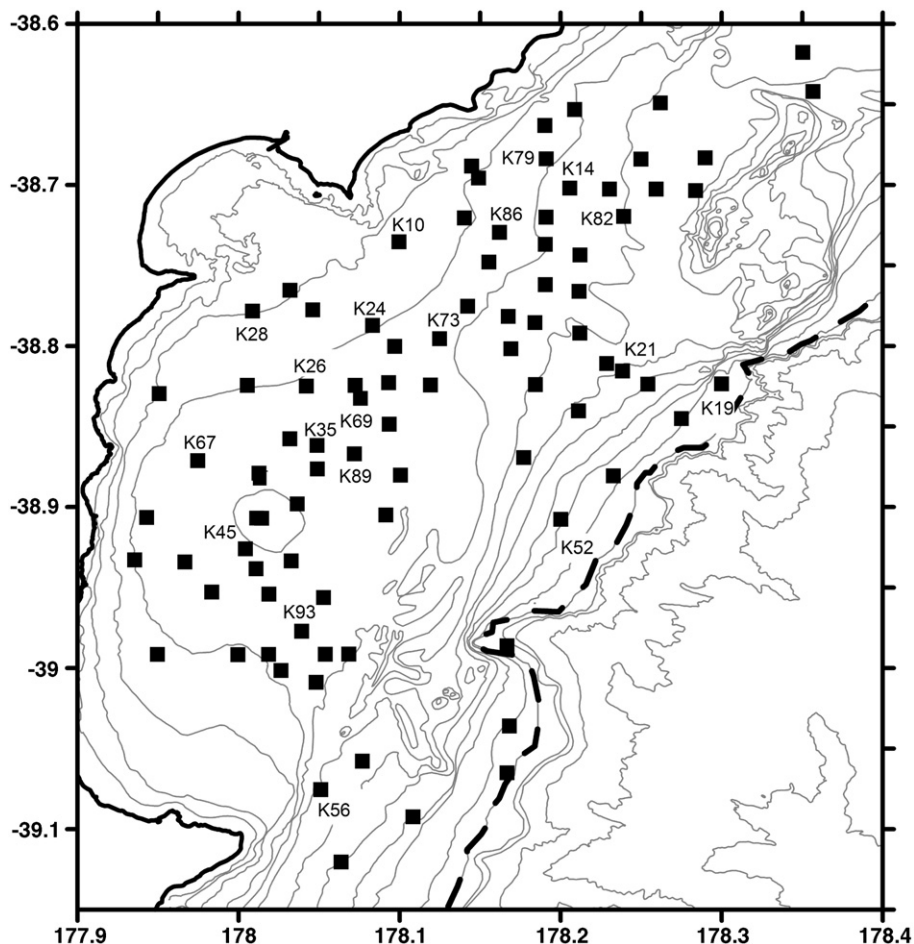


Fig. 2. Locations of kasten cores (black squares) collected on the Poverty shelf in January, 2005 using the *R/V Kilo Moana*. In total, 85 kasten cores were collected. All cores mentioned in text are labeled by core number. Dashed line indicates shelf break at 150 m.

depth increased. Sub-cores were removed for X-radiographic analysis to provide information on sedimentary structure.

3.2. Laboratory techniques

Analyses for ^{210}Pb were performed on all 85 kasten cores to calculate sediment accumulation rates. ^{210}Pb is a naturally occurring radioisotope in the ^{238}U decay series and has a half-life of 22.3 yr. In this analysis, the ^{210}Po daughter was measured by alpha spectrometry as a proxy for ^{210}Pb (assuming secular equilibrium) using the procedure described in Nittrouer et al. (1979). The only variation in our procedure was the use of a ^{209}Po spike instead of a ^{208}Po spike.

Supported ^{210}Pb activities varied across the study region; therefore supported levels of ^{210}Pb were estimated for each core by averaging the activities at depths displaying low and uniform activity, where excess activities had decayed to negligible levels. Accumulation rates were calculated using the slope of the ^{210}Pb excess activity profile for the region of the profile exhibiting logarithmic decrease with depth.

As biological and physical mixing can affect the ^{210}Pb gradient and hence interpretation of the accumulation rate, a second radioisotope was used in this study to verify ^{210}Pb -derived rates. Commonly, bomb-produced ^{137}Cs is used to verify ^{210}Pb rates; however, the low atmospheric fallout of bomb-produced radionuclides in the southern hemisphere has resulted in ^{137}Cs activities that are too low to detect by traditional methods (Kniskern, 2007). For this study, $^{239,240}\text{Pu}$ measured by Inductively Coupled Mass Spectrometry (ICP-MS) were used as alternatives to ^{137}Cs . Like ^{137}Cs , $^{239,240}\text{Pu}$ are bomb-produced radionuclides associated with atmospheric testing of nuclear weapons. ^{239}Pu and ^{240}Pu have half-lives of $24,110 \pm 30$ and 6564 ± 11 yr respectively. Profiles for $^{239,240}\text{Pu}$ are similar to those for ^{137}Cs in that they show a peak associated with the 1963/1964 fallout maximum, rather than a logarithmic decay profile as seen with ^{210}Pb . The accumulation rate can then be calculated by dividing the distance between the surface of the core and the $^{239,240}\text{Pu}$ peak (minus the mixed-layer thickness), by the time elapsed since maximum global fallout in 1963/1964.

Five cores were chosen for $^{239,240}\text{Pu}$ analysis based on the location and ^{210}Pb activity profile of the core. $^{239,240}\text{Pu}$ activity profiles for these cores were determined using the method described by Ketterer et al. (2004b). Samples were spiked with a ^{242}Pu solution and acid leached with HNO_3 . The remaining solvent was then filtered and the oxidation state was adjusted to Pu (IV) with NaNO_2 . TEVA resin was used for column chemistry. The column was rinsed with HNO_3 and HCl to remove U and Th from the sample. The Pu fraction was eluted with aqueous ammonium oxalate. These samples were run at Northern Arizona University. This method using the ICP-MS is more efficient, accurate, and sensitive than the traditional methods of alpha or gamma ray spectrometry (Ketterer et al., 2004a; Kim et al., 2000). The detection limit for the $^{239,240}\text{Pu}$ analysis is three times the standard deviation of the blank samples; for our sediment samples this amounts to a detection limit of $0.0014 \text{ dpm g}^{-1}$.

Grain-size analyses were performed on samples from two kasten cores exhibiting non-steady-state ^{210}Pb activity profiles to identify the possibility of grain-size influence on ^{210}Pb activities. The sand fraction of each sample was separated from the silt and clay by wet sieving. Pipette analysis (Gee and Bauder, 1986) was used to quantify the silt and clay fractions.

4. Results

4.1. Radiochemical data

Three main patterns of ^{210}Pb activity profiles have been identified on the shelf: steady-state profiles characterized by a logarithmic decrease with depth; profiles with uniform, low total activities, and non-steady-state profiles exhibiting fluctuating ^{210}Pb activity with depth (Fig. 3).

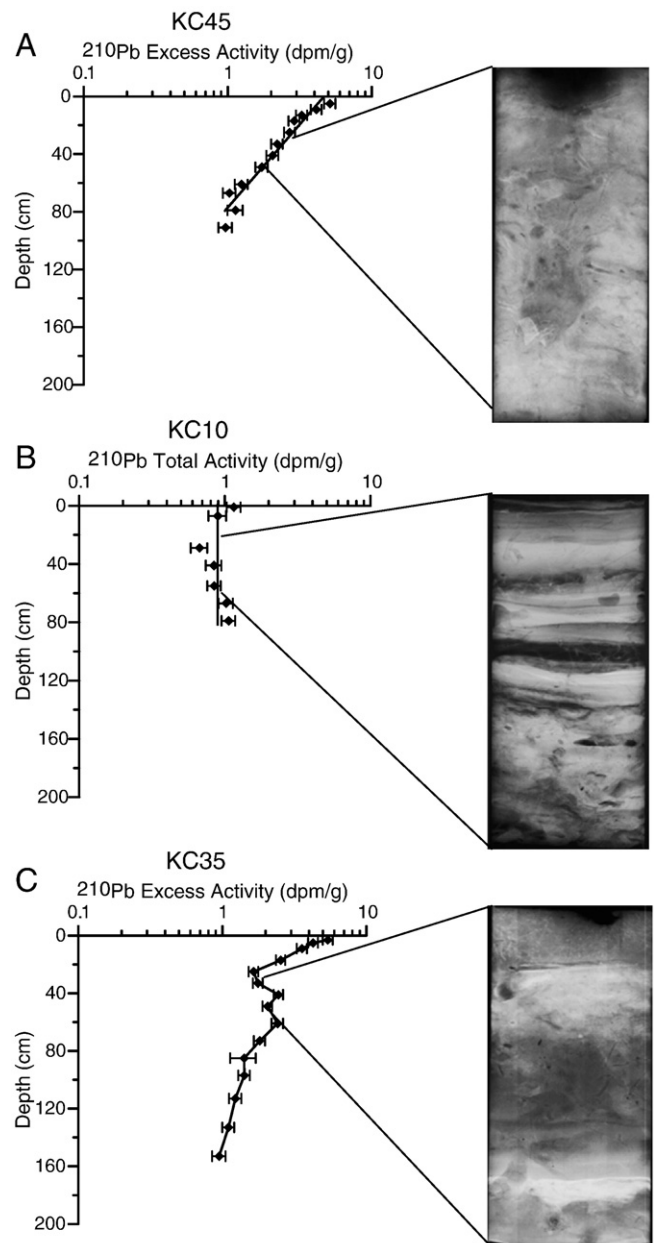


Fig. 3. Characteristic ^{210}Pb profiles for steady-state (A), low, uniform activity (B), and non-steady-state conditions (C). The solid line in each profile represents the linear regression (A), average activity (B), and a linear interpolation between points (C). X-radiographs (negatives) are 30 cm in length and represent the 30–60 cm interval in each core.

The steady-state profiles are located on the middle (40–70 m water depth) and outer shelves (70–150 m water depth) and the penetration depths of excess ^{210}Pb activity range in length from 20–175 cm (Figs. 3A–5). In most cases, a greater excess ^{210}Pb penetration depth will correspond with a higher accumulation rate. On the shallow mid-shelf (40–50 m water depth) located directly off Poverty Bay, profiles have very short excess ^{210}Pb activity penetration (usually less than 50 cm) and commonly exhibit accumulation rates less than 0.5 cm yr^{-1} (Fig. 5). Most cores on the northern and southern mid-shelf, landward of the anticlines, are characterized by steady-state profiles as well. These cores have much longer ^{210}Pb excess activity profiles and exhibit accumulation rates between 0.5 and 1.5 cm yr^{-1} (Fig. 5). Eleven of the cores in these two regions show a 5–10 cm zone of nearly uniform activity at the surface indicating the presence of a surface mixed layer resulting from biological or physical mixing. The

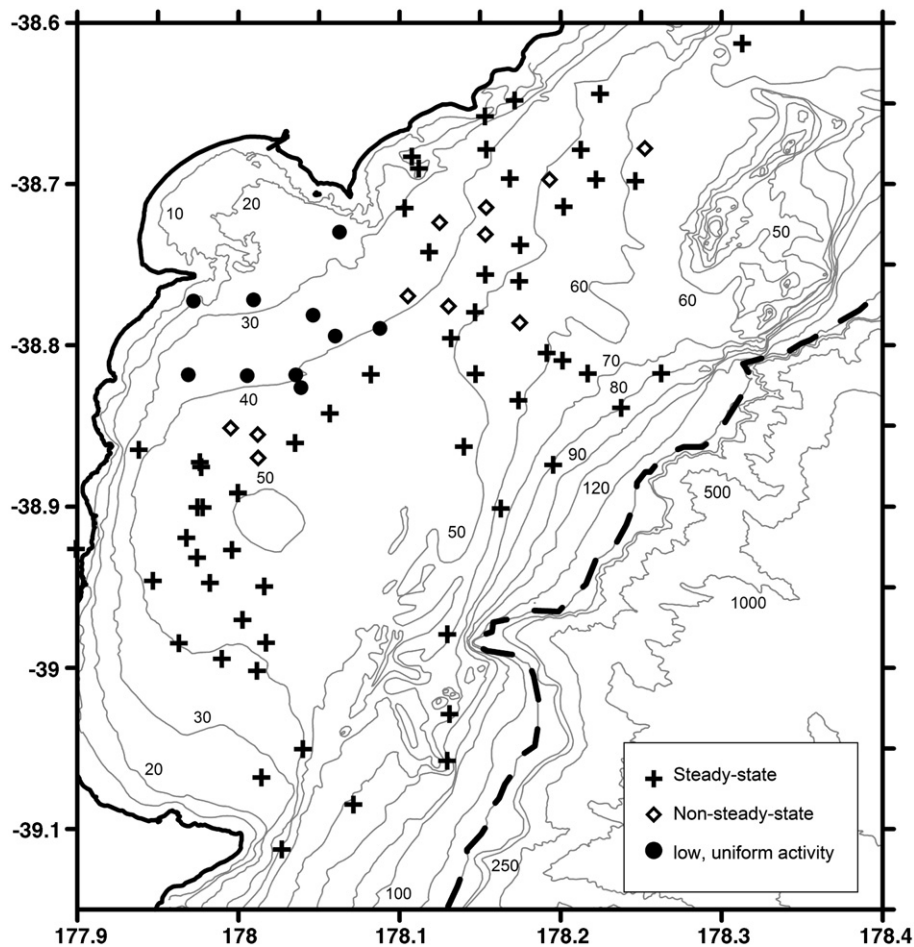


Fig. 4. Locations of three characteristic ^{210}Pb activity profiles (see Fig. 3). Profiles exhibiting low, uniform activities are found exclusively on the inner shelf; steady-state cores are found on the mid-shelf and outer shelf; and non-steady-state cores are located primarily in the mid-shelf depocenters. Dashed line indicates shelf break at 150 m.

cores located on the outer shelf (70–150 m water depth) are also characterized by steady-state excess activity profiles with accumulation rates ranging from $0.25\text{--}1.0\text{ cm yr}^{-1}$ (Fig. 5). The steady-state profiles often correlate with X-radiographs dominated by mottling and fewer laminations.

The majority of cores on the inner shelf, off Poverty Bay, tend to be short (<50 cm) with fairly uniform ^{210}Pb total activities around 1 dpm g^{-1} which is within the range ($0.5\text{--}1.2\text{ dpm g}^{-1}$) of supported ^{210}Pb activities found elsewhere on the shelf (Figs. 3B–5). The X-radiographs of these cores tend to show laminated facies with little evidence of biological mixing. This area of the shelf is also characterized by a high bulk density indicating it has a higher sand fraction (Rose and Kuehl, 2009-this issue).

The non-steady-state cores exhibit a general logarithmic decrease interrupted by layers of lower activity, and are found in the two depocenters landward of the anticlines (Figs. 3C–5). The majority of these cores exhibit relatively long excess activity penetration depths (>50 cm) and have apparent accumulation rates (estimated from the slope of the linear regression) similar to the surrounding steady-state cores.

Activity profiles for $^{239,240}\text{Pu}$ are characteristic of bomb-produced radionuclides, with activities increasing to maximum values corresponding with the 1963 maximum fallout and then decreasing upward to the surface (Fig. 6). The maximum activity peaks for all five kasten cores exhibit activities ranging from $0.015\text{--}0.02\text{ dpm g}^{-1}$.

4.2. Grain size

Grain-size analyses were conducted on two non-steady-state cores (KC35 and KC86) to determine whether low-activity peaks in the

^{210}Pb data were related to changes in grain size. In the northern depocenter (KC86), the sediment is composed of 22–35% clay (Fig. 7), 45–70% silt, and 3–30% sand, with the largest percent of the sand fraction located at the surface and at a depth of 85–100 cm. In the southern depocenter (KC35), the clay sized fraction ranges from 25–70%, silt fraction ranges from 35–60%, and the sand fraction ranges from 0–10% with the largest percent of the sand fraction located at the surface.

5. Discussion

5.1. Sediment geochronology

Steady-state accumulation. Steady-state profiles of ^{210}Pb activity commonly exhibit three characteristic regions (e.g., Koide et al., 1973; Nittrouer et al., 1979). The first region is the surface mixed layer, in which sediments are reworked by biological and physical processes, resulting in a zone of nearly uniform excess activity. This zone is present in 11 of the steady-state profiles on the Poverty shelf. In cores where a surface mixed layer is present, its thickness is generally <10 cm, which is common for many continental shelves (e.g., Koide et al., 1973; Nittrouer et al., 1979; Sommerfield and Nittrouer, 1999). The second region displays a logarithmic decrease of excess activity down-core, as a function of accumulation rate and radioactive decay. The accumulation rate is calculated from the slope of the excess ^{210}Pb profile in the zone of logarithmic decrease. The lower region of the profile represents supported levels where ^{210}Pb has achieved secular equilibrium with ^{226}Ra .

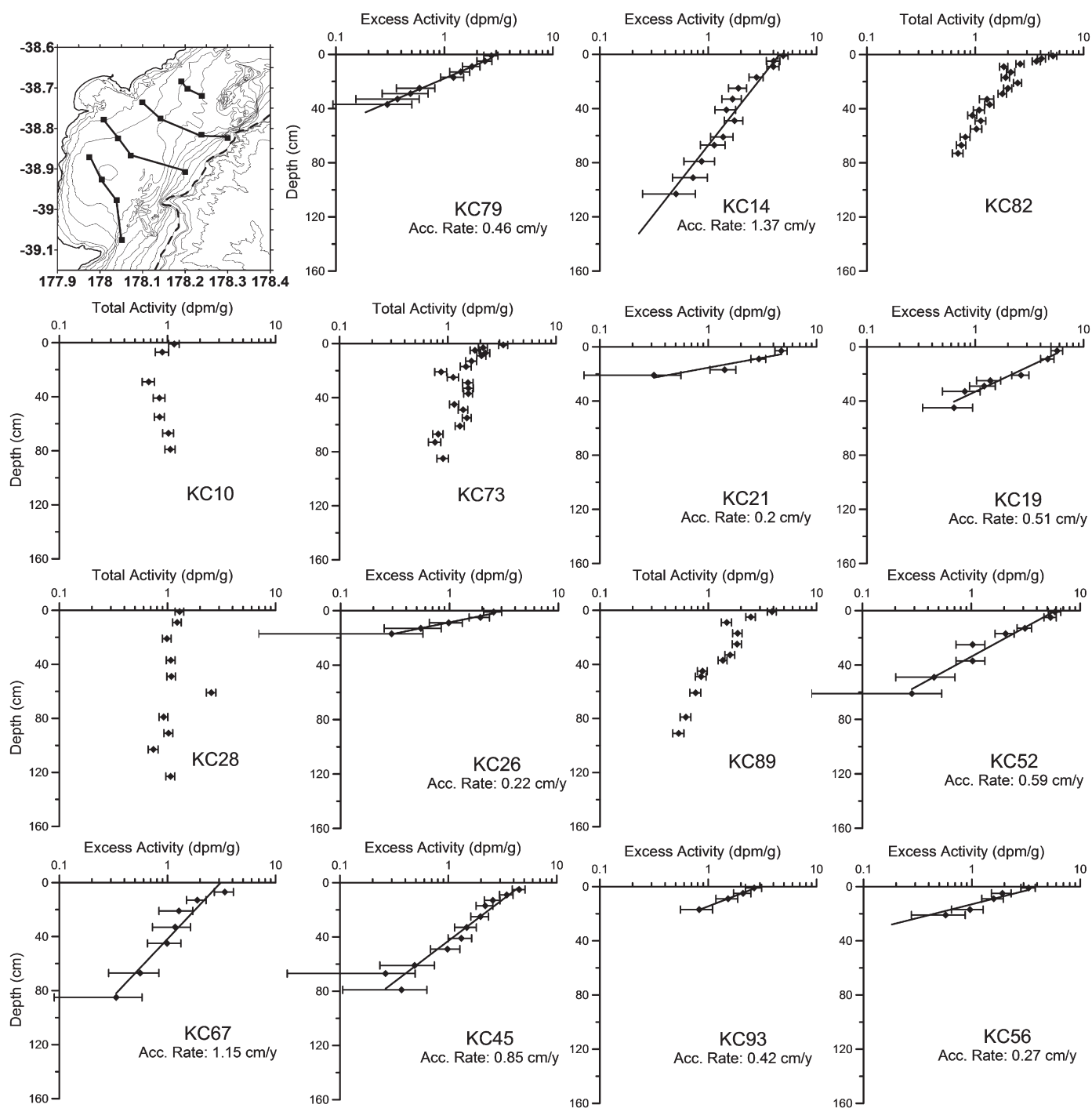


Fig. 5. Example ^{210}Pb profiles for the Poverty shelf. Excess activity profiles and calculated accumulation rates are shown for steady-state cores and total activity profiles are shown for non-steady-state cores and cores displaying low, uniform activity. ^{210}Pb profiles are oriented with North at the top of page and East at the left of page along transects as shown in inset.

The region of logarithmic decrease used to determine the accumulation rate could be affected by diffusive particle mixing, leading to an overestimation of accumulation rates. Therefore, ^{210}Pb accumulation rates are verified by the use of $^{239,240}\text{Pu}$. Activity profiles of $^{239,240}\text{Pu}$ are obtained for three cores displaying steady-state ^{210}Pb profiles and compared to accumulation rates calculated by the ^{210}Pb method (Fig. 6). Kasten core 14, located in the northern depocenter, shows a ^{210}Pb -derived accumulation rate of 1.37 cm yr^{-1} . This rate is used to estimate the 1963 (year of maximum fallout) depth. Depths of the surface mixed layer are added to the estimated depth to account for mixing. The ^{210}Pb rate indicates that the 1963 peak should occur at

approximately 57 cm which corresponds well with the maximum activity peak shown in the $^{239,240}\text{Pu}$ activity profile (Fig. 6). Kasten core 45, located in the southern depocenter, has an accumulation rate of 0.85 cm yr^{-1} which corresponds to a 1963 depth of 36 cm. Once again, the $^{239,240}\text{Pu}$ results show a maximum activity peak at this depth (Fig. 6). On the outer shelf, KC52 has a significant change in accumulation around 25 cm as seen by the change in the slope of the linear regression. The accumulation rate estimated from the excess activities spanning the entire length of the core is 0.59 cm yr^{-1} ; this is the value used for the shelf sediment budget. A significant change in accumulation rate is not seen in any other cores on the shelf. The

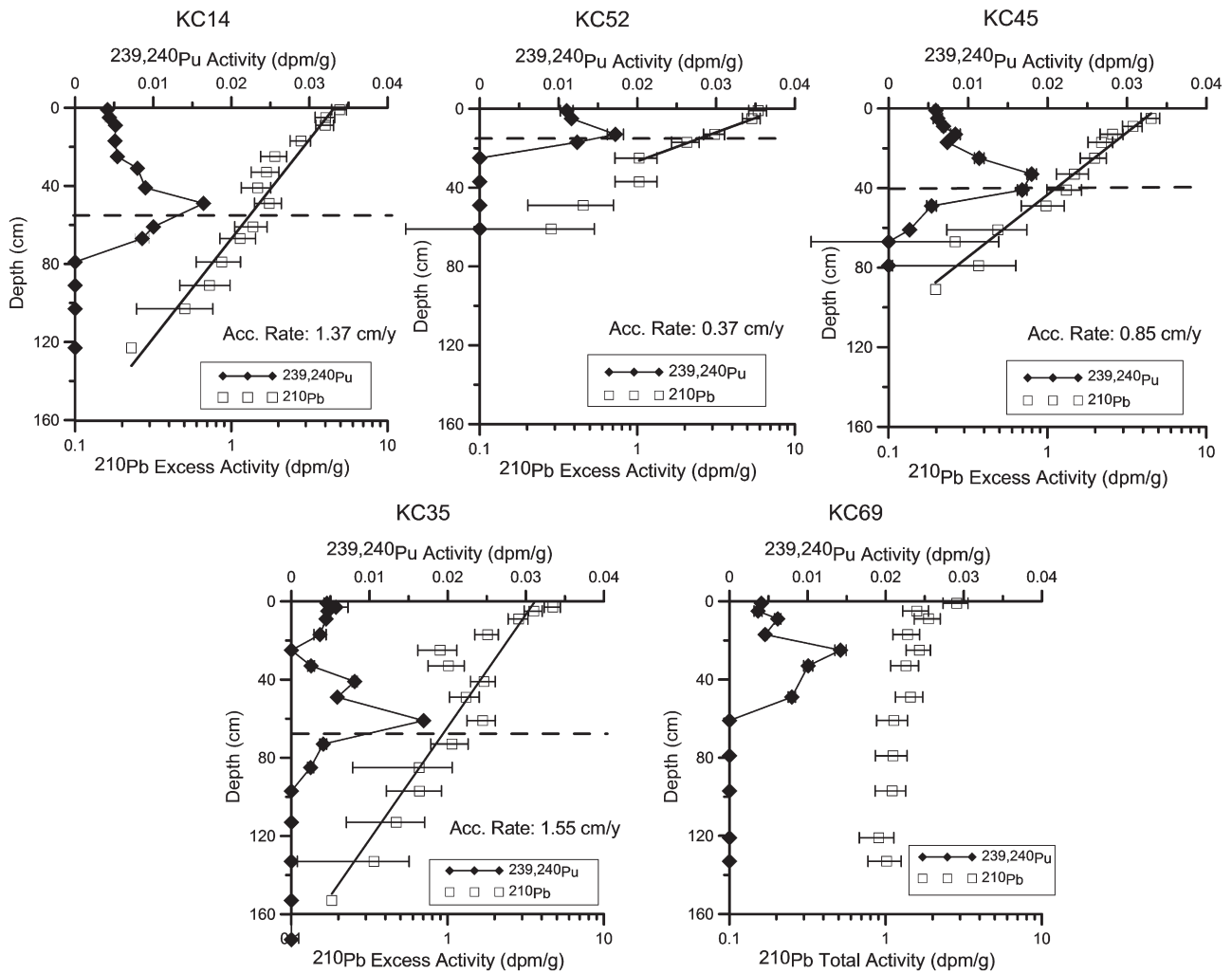


Fig. 6. $^{239,240}\text{Pu}$ and ^{210}Pb profiles for selected cores. Dashed line indicates 1963 maximum fallout date calculated from ^{210}Pb accumulation rates. Profiles for kasten cores 14, 52, 45, and 35 show that the depths of the 1963 maximum bomb fallout agree with ^{210}Pb derived accumulation rates. This concordance indicates minimal influence of diffusive mixing (i.e. bioturbation) on ^{210}Pb profiles and confirms accumulation rates calculated from the gradient of excess activity profiles. An accumulation rate could not be estimated in KC69 (see text for details).

calculated accumulation rate for the first 25 cm is 0.37 cm yr^{-1} with an R^2 value of 0.9775 and with a 1963 depth of 15.5 cm that corresponds with the $^{239,240}\text{Pu}$ peak (Fig. 6). In each of these cases, the estimated

and actual depths of the 1963 maximum fallout agree within a few centimeters, indicating that diffusive particle mixing beneath the surface mixed layer does not appreciably affect the ^{210}Pb profiles.

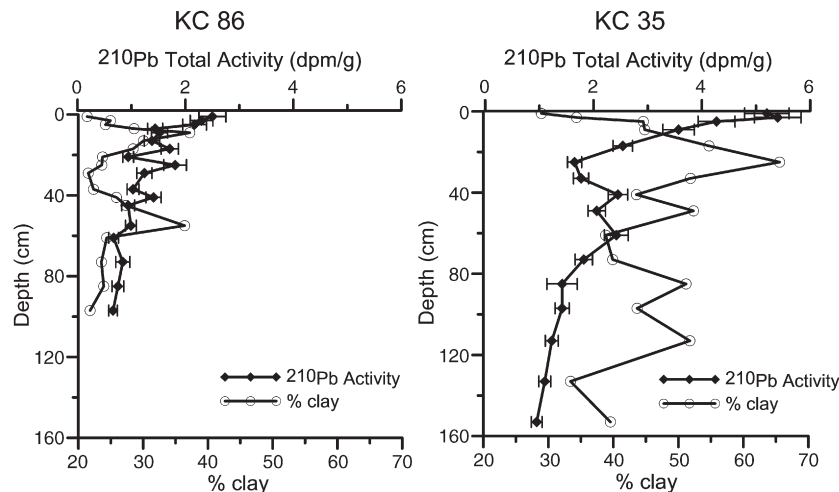


Fig. 7. ^{210}Pb activity profiles for cores KC86 and KC35 plotted against clay fraction. KC35 shows a potential correlation between low ^{210}Pb activity spikes and higher % clay indicating possible event deposition (see Fig. 8).

Low, uniform activities. A second common profile observed on the inner shelf and shallow mid-shelf (30–50 m) exhibits low activities (~ 1 dpm g^{-1}) which remain fairly uniform down-core (Fig. 3B). Low activities that are at levels supported by ^{226}Ra decay in sediments indicate non-depositional or erosional conditions. In some cases, uniform low activities are seen in the upper reaches of the core with a slight decrease to supported activities lower in the core. This characteristic can be associated with intense biological and/or physical mixing homogenizing the sediments (Dellapenna et al., 1998; Kuehl et al., 1986). A study of the grain-size distribution on the Poverty shelf by Foster and Carter (1997) indicates that fine sand is located on the inner shelf. A high sand fraction could lead to lower excess ^{210}Pb activities as a function of decreased particle surface area. On the inner Poverty shelf biological mixing is unlikely because X-radiographs of these cores show mostly laminated sediments with little evidence of bioturbation, therefore physical mixing may be responsible for these observed ^{210}Pb profiles (Fig. 3B). The absence of a logarithmic decrease layer suggests no net accumulation over the longer term, although the possibility that stochastic depositional events are preserved can not be ruled out.

Non-steady-state profiles. A few of the cores on the shelf exhibit non-steady-state, quasi-logarithmic decrease characterized by intermittent low-activity intervals (Fig. 3C). Such profiles have been observed by other researchers, and three possible explanations for these non-steady-state profiles have been suggested. The first assumes that the residence time of particles in the water column is constant, but that particles may have a different affinity for ^{210}Pb based on the grain size, mineralogy, and/or organic carbon content (Dukat and Kuehl, 1995; Kuehl et al., 1986; Nittrouer et al., 1979). The second explanation assumes that all particles have the same affinity for ^{210}Pb , but the residence time of particles in the water column is variable (e.g. Demaster et al., 1986; Kuehl et al., 1986). The third explanation is that abnormally high suspended-sediment concentrations can quickly deplete available dissolved oceanic ^{210}Pb , resulting in low-activity layers being emplaced in the sediments. For example, during flood events of the Eel River, sediment layers that have high clay content and low excess ^{210}Pb activity have been documented (Sommerfield and Nittrouer, 1999).

In this study, it is unlikely that the non-steady-state condition results from changes in mineralogy, because presumably all of the sediments originate from the Waipaoa catchment making high-frequency variations in mineralogy unlikely. Organic carbon content is

also not likely to affect the ^{210}Pb activity profiles because fairly uniform carbon content is seen throughout the shelf (Miller, 2008). It is also unlikely that the non-steady-state condition results from changes in grain size because a positive correlation between increasing ^{210}Pb activities and fine-grained sediment content was not observed (Fig. 7). On the contrary, grain-size analysis of KC35 indicates that low ^{210}Pb activity could be due to deposition of fine-grained flood event layers (Figs. 7,8) (Wheatcroft et al., 1997; Wheatcroft and Borgeld, 2000). In this case, ^{210}Pb excess activities have been corrected to eliminate the effect of decay on activities (Fig. 8). This has been accomplished by dividing the depth of the sample by the estimated accumulation rate to obtain the age of the sample. The decay-corrected activity has been calculated by incorporating the measured excess activity, age of the sample and the decay constant into the radioactive decay equation. An inverse correlation between % clay and decay-corrected ^{210}Pb excess activity shows an R^2 value of 0.61 (Fig. 8). However, a similar correlation for KC86 (R^2 value of 0.023) was not observed (Fig. 7), suggesting that flood events are not always responsible for observed variations.

Two non-steady-state cores were analyzed for $^{239,240}Pu$ as well as ^{210}Pb . One (KC35 located in the southern depo-center), exhibits a quasi-logarithmically decreasing ^{210}Pb profile interrupted by peaks of low activity and the other (KC69) has a stepped ^{210}Pb profile with low activity. An apparent accumulation rate of 1.55 $cm\ yr^{-1}$ has been determined for KC35 by using the slope of the linear regression including the low-activity peaks. The 1963 depth calculated from this rate corresponds with the maximum activity in the $^{239,240}Pu$ profile (Fig. 6). KC69 exhibits maximum activity at 33 cm below the surface of the core which equates to an apparent accumulation rate of 0.59 $cm\ yr^{-1}$. However, it is not possible to determine an accumulation rate for KC69 from the ^{210}Pb analysis so no correlation between ^{210}Pb and $^{239,240}Pu$ activities can be made (Fig. 6).

5.2. Accumulation rate trends

Characteristics of the ^{210}Pb activity profiles and their calculated accumulation rates change both along-shelf and across-shelf (Figs. 5,9). On the inner-to mid-shelf (30–50 m water depth) off Poverty Bay, the majority of the cores display low, uniform ^{210}Pb activities suggesting little net accumulation. In the shallow waters of the inner shelf, fine-grained sediments can often be reworked by intense waves and currents as indicated by the interlaminated facies. It is likely that these sediments

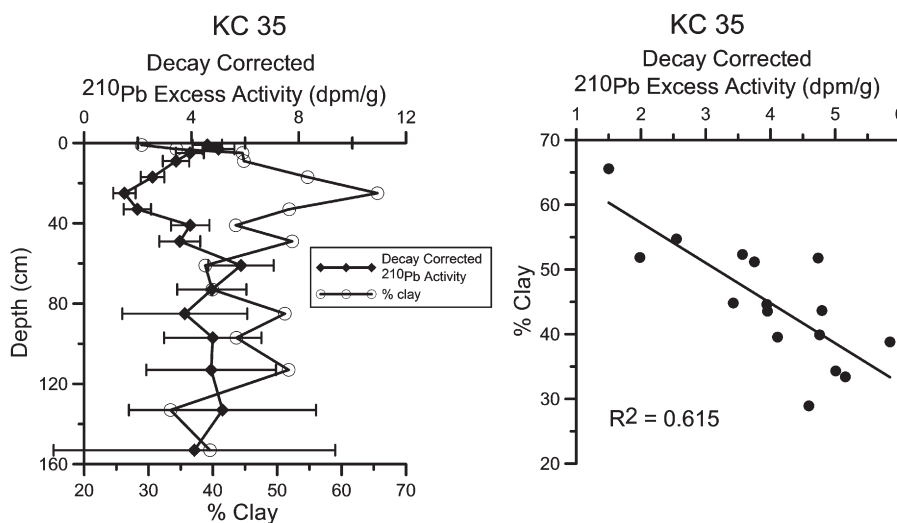


Fig. 8. Percent clay and decay-corrected ^{210}Pb excess activity for KC35 (left). Correlation between ^{210}Pb activity and % clay (right). In both graphs, the ^{210}Pb excess activities have been corrected using a linear depth-time conversion to eliminate the effect of radioactive decay. An inverse correlation between % clay and corrected ^{210}Pb activity shows an R^2 value of 0.615. This may indicate flood event deposition when ^{210}Pb -poor sediment is rapidly deposited.

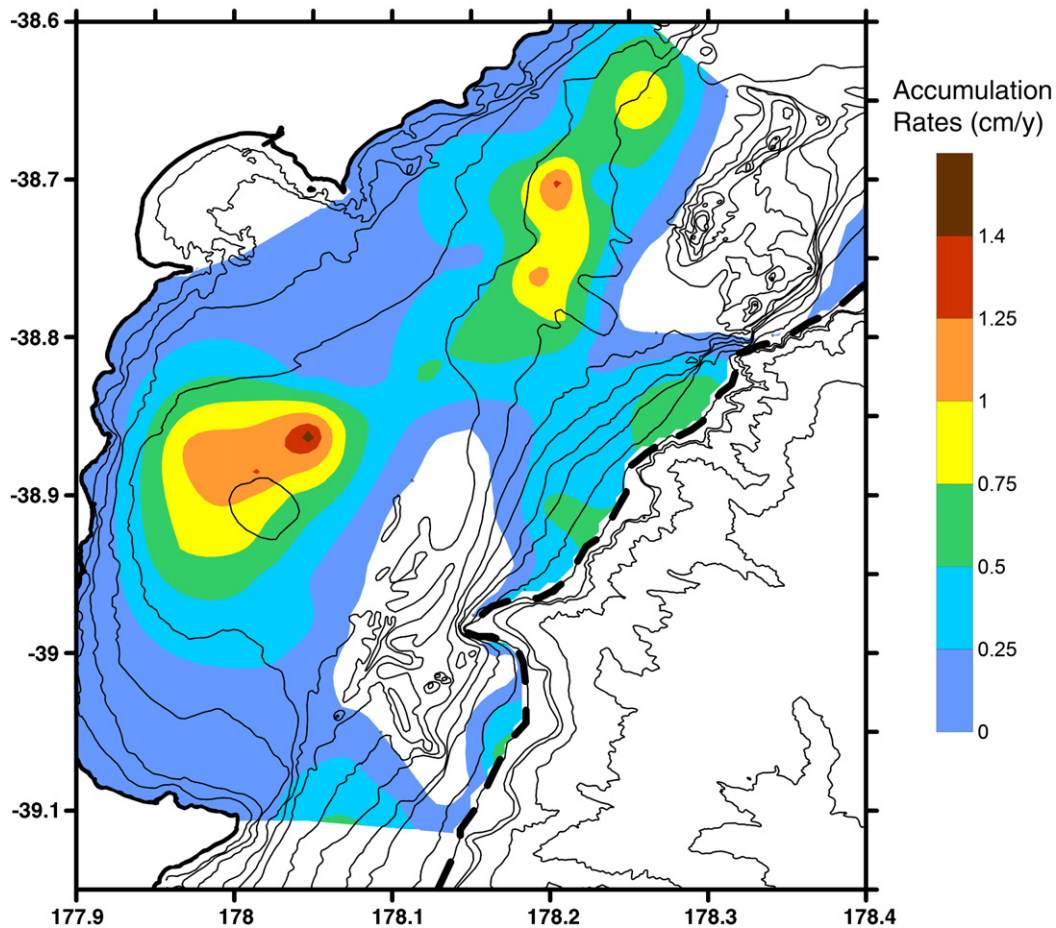


Fig. 9. Spatial distribution of ^{210}Pb accumulation rates (cm y^{-1}). Highest accumulation rates are seen in the northern and southern mid-shelf depocenters and along the shelf break. The highest accumulation rate found on the shelf is 1.5 cm y^{-1} . An estimated $3.6 \pm 0.9 \times 10^6 \text{ t yr}^{-1}$ of sediment is accumulating on the shelf which corresponds to 18–30% of the sediments discharged from the Waipaoa River. Regions without color indicate area outside of boundaries for the budget or represent anticlines where sediment cover is negligible.

are resuspended and transported to other locations on the shelf. Therefore, this region may be acting as a bypassing zone in which sediments are continually being removed and dispersed to other portions of the system rather than accumulating over a decadal timescale. This interpretation is also supported by bulk density measurements (Rose and Kuehl, 2009-this issue). This “bypassing region” is characterized by higher than average bulk densities indicating that there is a larger percentage of coarse silt and sand-size material located in this area, suggesting that the bulk of the fine sediments is dispersed to other locations.

Accumulation rates on the mid-shelf (40–70 m water depth and landward of the anticlines) increase to the north and south. The cores in these regions commonly exhibit steady-state ^{210}Pb profiles with only a few cores exhibiting the non-steady-state profiles. Therefore, it is possible to determine accumulation rates for most of the mid-shelf. These two areas exhibit the highest accumulation rates on the shelf, as high as 1.5 cm yr^{-1} , and seem to be the primary depocenters. These regions are also characterized by lower than average bulk densities indicating that these are loci of recent mud deposits (Rose and Kuehl, 2009-this issue). A likely explanation for the presence of these two depocenters is that the mid-shelf, landward of the Lachlan and Ariel anticlines, is experiencing subsidence at a rate of approximately 2 mm yr^{-1} , creating synclinal basins that provide accommodation space for the deposition of fluvial sediments (Foster and Carter, 1997).

The outer shelf, extending from 70 m water depth to the shelf break, is characterized by steady-state ^{210}Pb profiles with accumulation rates ranging from 0.25 to 1.0 cm yr^{-1} . This suggests that sediments are being transported between or across the Ariel and Lachlan

anticlines and are being deposited in a depocenter located along the shelf break. High accumulation along the shelf break suggests that a portion of the sediments may be reaching the continental slope. Recent results from Alexander et al. (2009-this issue) indicate that modern sediments are in fact accumulating on the Poverty slope.

5.3. Sediment budget

A modern (100-yr) bulk sediment budget for the Poverty shelf has been constructed from the distribution of ^{210}Pb accumulation rates. The budget includes the continental shelf extending from the 30-m isobath to the shelf break located around 140–170 m water depth. The northern boundary is defined as the bathymetric high associated with the Monowai Rocks. The southern boundary is defined as a line extending from the Mahia Peninsula to the shelf break at approximately $39^{\circ}07'\text{S}$ (Fig. 9).

For budget calculations, the shelf is divided into sub-regions based on 0.25 cm yr^{-1} differences in ^{210}Pb accumulation rates. The midpoint value of the apparent ^{210}Pb accumulation rates for each sub-region has been multiplied by an average dry bulk density value of 0.8 g cm^{-3} (Orpin et al., 2006) and integrated over the entire area to obtain the mass of sediments accumulating in each of these regions. This results in a value of $3.6 \times 10^6 \text{ t yr}^{-1}$. Even though accumulation rates obtained from $^{239,240}\text{Pu}$ corroborate the ^{210}Pb accumulation rates; this rate could be considered a maximum estimate due to possible influence from deep biological mixing as $^{239,240}\text{Pu}$ has not been measured in all cores. Most of these sediments are accumulating in two depocenters located on the mid-shelf landward of the anticlines and one

depo-center bordering the shelf break. The inner shelf, off Poverty Bay, accounts for much less of the sediment budget as it seems to be a bypassing region.

The possible errors associated with this budget include: (1) errors in the individual accumulation rate measurements, (2) limited spatial resolution of accumulation rates due to the sampling scheme and the inability to calculate accumulation rates for non-steady-state cores, (3) the use of an average bulk density value for the entire shelf, and (4) variable sediment discharge from the river.

The error for the individual accumulation rates has been estimated from the standard error of the slopes calculated from the ^{210}Pb profiles. The average error of the slope estimated from all cores results in a 25% uncertainty for the accumulation rates. This equates to an uncertainty of approximately $0.9 \times 10^6 \text{tyr}^{-1}$ in the overall sediment budget.

Error associated with the spatial resolution of ^{210}Pb data and thus the contouring for the sediment budget, is not easily quantified. The sampling scheme for this project provides fairly good spatial resolution for the mid-shelf and outer shelf but poorer resolution near-shore and near the anticlines. The inner shelf and coastline is composed of mostly sandy sediments (Foster and Carter, 1997) and thus likely would not greatly contribute to the sediment budget. Similarly, the anticlines are topographic highs that have negligible sediment cover based on seismic data (Gerber et al., 2009–this issue; Kuehl et al., 2006) and therefore omission of the anticlines from the overall budget should have a negligible effect.

The above budget estimate includes ^{210}Pb rates from 70 out of the 85 profiles measured. Cores exhibiting non-steady-state conditions for which a general logarithmic decrease is not apparent are excluded

from the budget. Accumulation rates for cores with low, uniform activities could not be calculated; therefore these cores are assigned a general accumulation rate of 0.1cmyr^{-1} . In an effort to extend the spatial resolution of accumulation-rate estimates, a second sediment budget has been calculated using the maximum penetration depths of ^{210}Pb (Fig. 10). Accumulation rates have been calculated by dividing the maximum penetration depth of ^{210}Pb excess activity (excluding the surface mixed layer depth) by the effective span of time represented by excess ^{210}Pb activity. As is the case for most radio-active decay schemes, ^{210}Pb geochronology is effective over a timescale of 4–5 times the isotope half-life. In this case, the depth of penetration is assumed to represent between 88 and 110 yr. The sediment budget calculated using this approach estimates that approximately $3.2\text{--}4.0 \times 10^6 \text{tyr}^{-1}$ of the sediment is retained on the shelf. This value supports our earlier estimate calculated from the accumulation rates of the steady-state cores.

The Waipaoa River discharge is currently estimated to be 15Mtyr^{-1} and is measured at a gauging station located at Kanakanaia Bridge, 48 km upstream from the river mouth. Currently, there is little data on the amount of sediment accreting on the flood plain between the gauging station and the river mouth. Therefore, the current discharge value should be considered a maximum estimate. Errors in the discharge estimate could also arise from the episodic nature of the river discharge due to reoccurring flooding from storms.

Based on the sediment budget, $3.6 \pm 0.9 \times 10^6 \text{tyr}^{-1}$ of river derived sediments is remaining on the shelf over the past 100 yr. This only amounts to between 18 and 30% of the total river discharge. The remaining sediments are likely leaving the shelf system or is being deposited before reaching the shelf. A small portion of

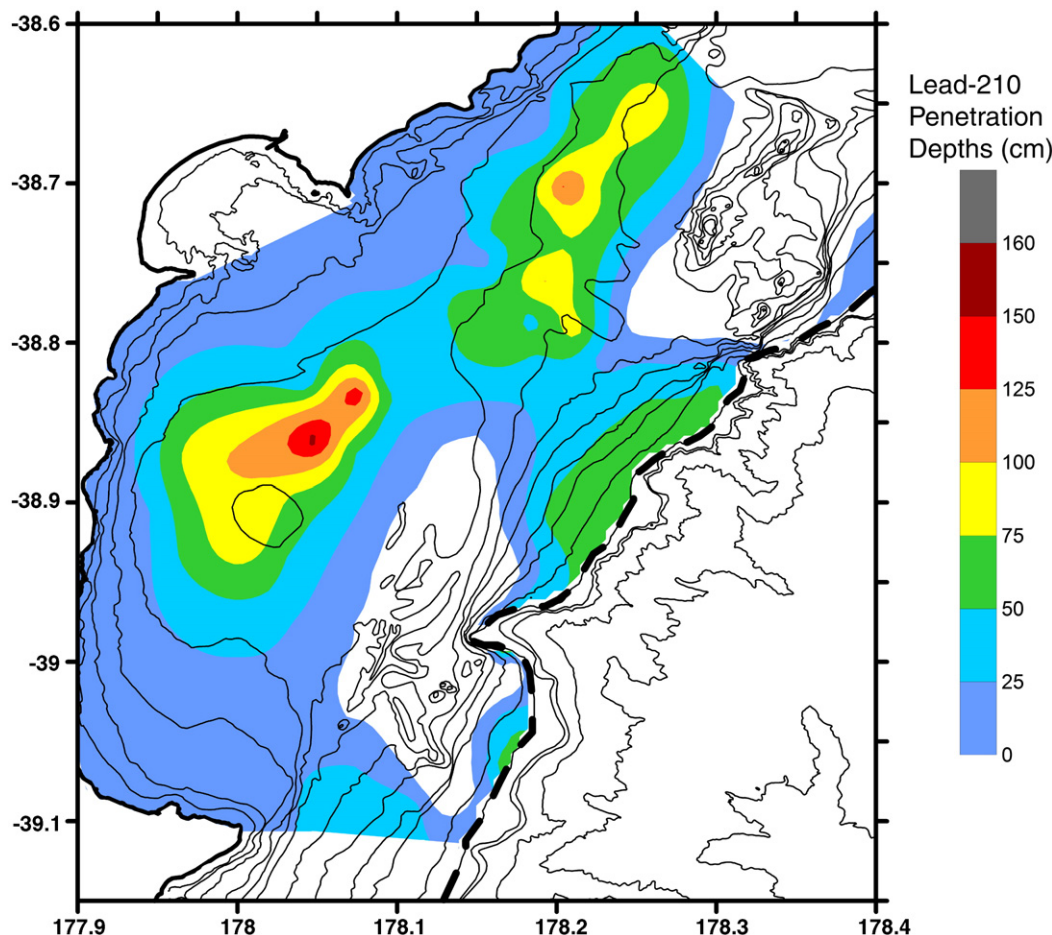


Fig. 10. Spatial distribution of ^{210}Pb penetration depths (cm) estimated from excess activity profiles. Depocenters are seen on the northern and southern mid-shelf regions and along the shelf break. ^{210}Pb penetration depth data is used to estimate that 21.5–26.5% of the sediments discharged from the Waipaoa is retained on the shelf (see Discussion).

sediments may be trapped on the floodplain. During flooding events, sediments can breach the levees along the lower reaches of the Waipaoa River and accumulate on the floodplain. It is also likely that a portion of the sediments are being captured within Poverty Bay, which is not included in this budget. A portion of the remaining sediments could be transported to the north past the Monowai Rocks by the Wairarapa Coastal Current, which has a net northward flow. Moderate ^{210}Pb accumulation rates ($0.25\text{--}0.5\text{ cm yr}^{-1}$) calculated from cores in this area indicate that this is a possible sediment dispersal pathway. Moderate ^{210}Pb accumulation rates are also seen at the southern boundary of the budget near the Mahia Peninsula. Southward moving winds have been shown to move sediment plumes to the south around the tip of Mahia Peninsula (Foster and Carter, 1997). Therefore, sediments from the Waipaoa may also be transported south of the budget limits.

A large portion of the fluvial sediments is likely bypassing the narrow shelf and being deposited on the adjacent continental slope as indicated by the high accumulation of modern sediments along the shelf break. In fact, the highest accumulation rate (1.8 cm yr^{-1}) measured in this study is located in the canyon head just beyond the shelf break. It is likely that the canyons along the shelf break are important conduits for sediments leaving the shelf. Possible mechanisms for increasing accumulation at the shelf break and dispersing sediments to the slope include (1) hemipelagic sedimentation from buoyant plumes, (2) direct bypassing of the shelf by hyperpycnal plumes and wave-supported gravity currents, and (3) resuspension and dispersal of shelf sediments by waves and currents (Sommerfield and Nittrouer, 1999). A study by Alexander et al. (2009-this issue) indicates that approximately 15% of fluvial sediments are being deposited on the slope.

A distinctive characteristic of the Poverty shelf is the small portion of total fluvial sediments actually remaining on the shelf. Similar results have been seen in other tectonically active margins with subsiding mid-shelf basins. Sommerfield and Nittrouer (1999) constructed a sediment budget for the Eel River located off Northern California using ^{210}Pb geochronology. The ^{210}Pb data demonstrate that river derived mud accumulates from the 50 m isobath seaward and that the highest accumulation rates are present in areas associated with flood deposition. They have determined that a maximum of 20% of the sediments entering the system remains on the continental shelf in a mid-shelf depocenter similar to the depocenters associated with the Poverty shelf. The majority of Eel River sediments bypass the narrow continental shelf and are dispersed to the adjacent slope (Alexander and Simoneau, 1999). Similarly, studies of the Waiapu shelf also located on the east coast of the North Island, NZ exhibit the highest accumulations on the mid-to-outer shelf. A sediment budget of this region indicates that between 32 and 39% of fluvial load is retained on the shelf (Kniskern, 2007). In contrast, passive margin shelves adjacent to rivers such as the Amazon typically exhibit cliniform deposition rather than mid-shelf mud belts and retain more of the fluvially derived sediments on the shelf. For example, sediment budgets for the Amazon, Adriatic, and Canadian Beaufort shelves estimate that 40–70%, 90%, and 85% of sediments, respectively, is retained on these shelves (Kuehl et al., 1986; Frignani et al., 2005; Macdonald et al., 1998).

5.4. Long vs. short-term accumulation

Modern sedimentation patterns based on ^{210}Pb geochronology compare favorably with Holocene high-stand patterns obtained from seismic mapping in other studies of the Poverty shelf (Gerber et al., 2009-this issue; Kuehl et al., 2006; Orpin et al., 2006). In particular, the Holocene isopach depicts major depocenters for Holocene sediments located in subsiding synclinal basins landward of the anticlines and along the shelf break, with less sediment accumulation on the inner shelf and between the two anticlines (Gerber et al., 2009-this

issue). The largest contrast between the sedimentation patterns of these two timescales is that for modern sedimentation, the northern and southern depocenters are both equally significant repositories for sediments (Fig. 9). The modern budget also indicates that the outer shelf depocenter is not as significant a repository as the two mid-shelf depocenters. The Mid-Late Holocene budget (5530 YBP-present) from Gerber et al. (2009-this issue) indicate that the southern mid-shelf basin is the primary depocenter containing 60–65% of the total estimated sediment deposit.

Gerber et al. (2009-this issue) suggest that the discrepancy between the sediment infilling of the two mid-shelf basins is a result of differential subsidence. Acoustic reflectors in the southern depocenter define an underfilled synclinal basin in which the accommodation space seems to be greater than the fluvial sediment supply. Reflectors in the northern depocenter show a more progradational pattern which Gerber et al. (2009-this issue) suggest results from sediment supply being greater than the accommodation space created by subsidence.

One possible explanation for the similarity between the northern and southern depocenters in the modern budget may be that the subsidence rate in the northern depocenter has recently increased as a result of recent coseismic subsidence. Earthquake related displacement has occurred at least six times in the Hawke's Bay region (directly south of the Waipaoa Basin) over the last 7200 yr with a net subsidence of 7 m (Hayward et al., 2006). Another possible explanation for the similarity between depocenters in the modern budget may result from the recent increase in fluvial sediment supply. The six-fold increase in sediment yield (Gerber et al., 2009-this issue; Page et al., 2001; Wilmshurst et al., 1999) may have changed the southern depocenter from a supply- to an accommodation-limited system. In this case, both mid-shelf depocenters would be accommodation-limited and sediments would likely accumulate at the same rate in both.

Tectonic influence on Holocene and modern sedimentation is also seen on other active margins such as the Eel River margin in northern California. Like the Poverty shelf, Holocene sedimentation on the Eel shelf is characterized by high sediment accumulation in a subsiding synclinal basin on the mid- to outer shelf (Sommerfield and Nittrouer, 1999). Sommerfield and Nittrouer (1999) also report findings that modern (100-yr) accumulation from ^{210}Pb analysis generally occurs over these same regions of thick Holocene deposits.

Gerber et al. (2009-this issue) estimate that 1.5–2.5 Mt of sediments per year has accumulated on the shelf during the last 5530 yr. Kettner et al. (2007) estimate a sediment discharge of $2.3 \pm 4.5\text{ Mtyr}^{-1}$ for the past 3000 yr using HydroTrend; a numerical model that determines water and suspended-sediment discharge as a function of climate and catchment characteristics. A sediment discharge of 2.3 Mtyr^{-1} and a Mid-Late Holocene shelf capture of $1.5\text{--}2.5\text{ Mtyr}^{-1}$ indicate that the shelf may have had a high trapping efficiency (Gerber et al., 2009-this issue). A comparison of the Late-Holocene budget with the modern (100-yr) budget indicates an increase between a factor of 1.5 and 2.5 in the sedimentation rate. However, the riverine sediment supply is estimated to have increased by a factor of six since the settlement, and subsequent deforestation, of the Waipaoa catchment (Gerber et al., 2009-this issue; Kettner et al., 2007). This suggests that the shelf has evolved from a shelf with a high trapping efficiency (Gerber et al., 2009-this issue) to a system in which much of the riverine sediment is bypassing the shelf due to the sediment load exceeding the tectonically produced accommodation space. In this system, human activities have greatly altered sedimentation in a relatively short amount of time. Since continental margins are important sediment repositories due to their rich record of Earth history, mineral and energy resources, and large carbon sequestration, any changes in sedimentation from natural or human impacts could have potential implications for these margin processes.

There are many uncertainties when comparing sedimentation rates over different timescales. Not only can fluvial loads be

significantly different due to climate shifts, tectonics, and land-use changes; but the oceanographic conditions on the margin can also change, leading to differences in the ability to retain sediments on the shelf (Goodbred and Kuehl, 1999). Another potential problem in the comparison of sedimentation rates over different timescales results from hiatuses in the sedimentary record, which can be attributed to periods of non-deposition or erosion. Hiatuses typically cause accumulation rates to be time-variant; the rates decrease with an increase in the time measured due to greater likelihood of stratigraphic incompleteness (Sadler, 1981). However, this so-called “Sadler effect” is not evident on the Poverty shelf, especially considering that a factor of six increase in sediment input has only resulted in a factor of two increase in shelf accumulation relative to the Mid-Late Holocene average. These observations further support the idea that the shelf is presently accommodation-limited and that a large fraction of the modern Waipaoa sediments delivered to the shelf escapes the study area.

6. Conclusions

The major conclusions of this paper are summarized below.

- (1) Three characteristic ^{210}Pb activity profiles are seen on the Poverty shelf. Low, uniform activity profiles for the inner shelf likely result from physical mixing and resuspension of sediments by energetic waves and currents. Steady-state profiles are observed in the northern and southern depocenters and on the outer shelf. Non-steady-state ^{210}Pb activity profiles occur in the two mid-shelf depocenters. These non-steady-state profiles likely result from event deposition or changes in particle residence times.
- (2) Fine-grained sediments from the Waipaoa seem to be bypassing the inner shelf and being primarily deposited in two mid-shelf depocenters located in the subsiding synclinal basins landward of the anticlines. A portion of the sediments is also being deposited on the outer shelf along the shelf break indicating that sediments may be reaching the slope.
- (3) A sediment budget indicates that $3.6 \pm 0.9 \times 10^6 \text{ t yr}^{-1}$ of sediments accumulates on the Poverty continental shelf. This amounts to only 18–30% of the total sediments discharged from the river. The remainder of the sediments is probably transported to the slope and/or out of the system to the north or south.
- (4) Modern sedimentation patterns are similar to Holocene patterns. This suggests that sediment deposition is mainly controlled by regional tectonics and shelf morphology rather than oceanographic forces.
- (5) Changing land-use practices and consequent increases in sediment discharge have forced a remarkable change in the functioning of the Poverty margin. In an instant of geologic time (i.e. <100yr) the entire margin has shifted from one of highly efficient shelf sediment capture to one where the majority of the material input from the river is escaping the adjacent shelf, with a significant portion being transported directly to the slope.

Acknowledgements

This research was supported by the NSF MARGINS Source-to-Sink program, OCE-0405524. We would like to thank our colleagues at NIWA and the crew of the R/V *Kilo Moana* for all of their assistance with the field work. We also thank Linda Meneghini, Lila Rose, and Lisa Addington for their help with the ^{210}Pb analysis and Michael Ketterer for his assistance with $^{239,240}\text{Pu}$ geochronology.

References

- Alexander, C.R., Simoneau, A.M., 1999. Spatial variability in sedimentary processes on the Eel continental slope. *Marine Geology* 154, 243–254.
- Alexander, C.R., Walsh, J.P., Orpin, A., 2009. This issue. Modern sediment dispersal and accumulation on the outer Poverty continental margin. *Marine Geology*.
- Berryman, K., Marden, M., Eden, D., Mazengarb, C., Ota, Y., Moriya, I., 2000. Tectonic and paleoclimatic significance of Quaternary river terraces of the Waipaoa River, East Coast, New Zealand. *New Zealand Journal of Geology and Geophysics* 43, 229–245.
- Carter, L., Carter, R.M., McCave, I.N., Gamble, J., 1996. Regional sediment recycling in the abyssal Southwest Pacific Ocean. *Geology* 24 (8), 735–738.
- Carter, L., Manighetti, B., Elliot, M., Trustrum, N., Gomez, B., 2002. Source, sea level and circulation effects on the sediment flux to the deep ocean over the past 15 ka off eastern New Zealand. *Global and Planetary Change* 33, 339–355.
- Clarke Jr., S.H., 1987. Late Cenozoic geology and structure of the onshore-offshore Eel River Basin, Northern California. In: Schymiczek, H., Suchsland, R. (Eds.), *Tectonics, Sedimentation and Evolution of the Eel River and Associated Coastal Basins of Northern California*. Miscellaneous Publication, vol. 37. San Joaquin Geological Society, pp. 31–40.
- Dellapenna, T.M., Kuehl, S.A., Schaffner, L.C., 1998. Sea-bed mixing and particle residence times in biologically and physically dominated estuarine systems: a comparison of Lower Chesapeake Bay and the York River subestuary. *Estuarine, Coastal and Shelf Science* 46 (6), 777–795.
- DeMaster, D.J., Kuehl, S.A., Nittrouer, C.A., 1986. Effects of suspended sediments on geochemical processes near the mouth of the Amazon River: examination of biological silica uptake and the fate of particle-reactive elements. *Continental Shelf Research* 6 (1–2), 107–125.
- Dukat, D.A., Kuehl, S.A., 1995. Non-steady-state ^{210}Pb flux and the use of $^{228}\text{Ra}/^{226}\text{Ra}$ as a geochronometer on the Amazon continental shelf. *Marine Geology* 125 (3–4), 329–350.
- Foster, G., Carter, L., 1997. Mud sedimentation on the continental shelf at an accretionary margin – Poverty Bay, New Zealand. *New Zealand Journal of Geology and Geophysics* 40, 157–173.
- Frignani, M., Langone, L., Ravaoli, M., Sorgente, D., Alvisi, F., Albertazzi, S., 2005. Fine-sediment mass balance in the western Adriatic continental shelf over a century time scale. *Marine Geology* 222–223, 113–133.
- Gee, G.W., Bauder, J.W., 1986. Particle-size analysis. In: Klute, A. (Ed.), *Methods of Soil Analysis: Part 1. Physical and Mineralogical Methods*, 2nd edn. Agronomy, vol. 9. Soil Science Society of America, Madison, USA, pp. 383–411.
- Gerber, T.P., Pratson, L.F., Kuehl, S.A., Walsh, J.P., Alexander, C., Palmer, A., 2009. This issue. The influence of sea level and tectonics on Late Pleistocene through Holocene sediment storage along the high-sediment supply Poverty continental shelf. *Marine Geology*.
- Gomez, B., Fulthorpe, C., Carter, L., Berryman, K., Browne, G., Green, M., Hicks, M., Trustrum, N., 2001. Continental margin sedimentation to be studied in New Zealand. *Eos, Transactions, American Geophysical Union*, 82 (14), 161, 166–167.
- Goodbred, S.L., Kuehl, S.A., 1999. Holocene and modern sediment budgets for the Ganges–Brahmaputra river system: evidence for highstand dispersal to flood-plain, shelf, and deep-sea depocenters. *Geology* 27 (6), 559–562.
- Griffiths, G.A., 1982. Spatial and temporal variability in suspended sediment yields of North Island basins, New Zealand. *Water Resources Bulletin* 8 (4), 575–583.
- Hayward, B.W., Grenfell, H.R., Sabaa, A.T., Carter, R., Cochran, U., Lipps, J.H., Shane, P.R., Morely, M.S., 2006. Micropaleontological evidence of large earthquakes in the past 7200 years in southern Hawke's Bay, New Zealand. *Quaternary Science Reviews* 25 (11–12), 1186–1207.
- Hicks, D.M., Gomez, B., Trustrum, N.A., 2000. Erosion thresholds and suspended sediment yields, Waipaoa River Basin, New Zealand. *Water Resources Research* 36 (4), 1129–1142.
- Hicks, D.M., Gomez, B., Trustrum, N.A., 2004. Event suspended sediment characteristics and the generation of hyperpycnal plumes at river mouths: East Coast Continental Margin, North Island, New Zealand. *The Journal of Geology* 112, 471–485.
- Ketterer, M.E., Hafer, K.M., Jones, V.J., Appleby, P.G., 2004a. Rapid dating of recent sediments in Loch Ness: inductively coupled plasma mass spectrometric measurements of global fallout plutonium. *Science of the Total Environment* 322, 221–229.
- Ketterer, M.E., Hafer, K.M., Link, C.L., Kolwaite, D., Wilson, J., Mietelski, J.W., 2004b. Resolving global versus local/regional Pu sources in the environment using sector ICP-MS. *Journal of Analytical Atomic Spectrometry* 19, 241–245.
- Kettner, A.J., Gomez, B., Syvitski, J.P.M., 2007. Modeling suspended sediment discharge from the Waipaoa River system, New Zealand: the last 3000 years. *Water Resources Research* 43, W07411. doi:10.1029/2006WR005570.
- Kim, C.S., Kim, C.K., Lee, J.L., Lee, K.J., 2000. Rapid determination of Pu isotopes and atom ratios in small amounts of environmental samples by an on-line sample pre-treatment system and isotope dilution high resolution inductively coupled plasma mass spectrometry. *Journal of Analytical Atomic Spectrometry* 15, 247–255.
- Kniskern, T.A., 2007. Shelf sediment dispersal mechanisms and deposition on the Waipaoa river shelf, New Zealand. Dissertation, School of Marine Science: the College of William and Mary.
- Koide, M., Bruland, K.W., Goldberg, E.D., 1973. Th-228/Th-232 and Pb-210 geochronologies in marine and lake sediments. *Geochimica et Cosmochimica Acta* 37, 1171–1187.
- Kuehl, S.A., Alexander, C.A., Carter, L., Gerald, L., Gerber, T., Harris, C., McNinch, J., Orpin, A., Pratson, L., Syvitski, J., Walsh, J.P., 2006. Understanding sediment transfer from land to ocean. *Eos, Transactions of the American Geophysical Union* 87 (29).
- Kuehl, S.A., DeMaster, D.J., Nittrouer, C.A., 1986. Nature of sediment accumulation on the Amazon continental shelf. *Continental Shelf Research* 6, 209–225.
- Lewis, K.B., Lallemand, S.E., Carter, L., 2004. Collapse in a Quaternary shelf basin off East Cape, New Zealand: evidence for passage of a subducted seamount inboard of the

- Ruatoria giant avalanche. *New Zealand Journal of Geology and Geophysics* 47, 415–429.
- Macdonald, R.W., Solomon, S.M., Cranston, R.E., Welch, H.E., Yunker, M.B., Gobeil, C., 1998. A sediment and organic carbon budget for the Canadian Beaufort shelf. *Marine Geology* 144, 255–273.
- Miller, A.J., 2008. A modern sediment budget for the continental shelf off the Waipaoa River, New Zealand. Thesis, School of Marine Science: the College of William and Mary.
- Milliman, J., Syvitski, J.P.M., 1992. Geomorphic/tectonic control of sediment discharge to the ocean: the importance of small mountainous rivers. *The Journal of Geology* 100, 525–544.
- Nittrouer, C.A., Sternberg, R.W., Carpenter, R., Bennett, J.T., 1979. The use of Pb-210 geochronology as a sedimentological tool: application to the Washington continental shelf. *Marine Geology* 31, 297–316.
- Orpin, A.R., Alexander, C., Carter, L., Kuehl, S., Walsh, J.P., 2006. Temporal and spatial complexity in post-glacial sedimentation on the tectonically active, Poverty Bay continental margin of New Zealand. *Continental Shelf Research* 26, 2205–2224.
- Page, M., Trustrum, N., Brackley, H., Gomez, B., Kasai, M., Marutani, T., 2001. Source-to-sink sedimentary cascades in the Pacific Rim geo-systems. In: Brierley, Gary J., Trustrum, Noel A., Mike, Page (Eds.), *Matsumoto Sabo Work Office, Ministry of Land, Infrastructure and Transport, Nagano, Japan*, pp. 86–100. 184 pp.
- Rose, L.E., Kuehl, S.A., 2009-this issue. Recent sedimentation patterns and facies distribution on the Poverty Shelf, New Zealand. *Marine Geology*.
- Sadler, P.M., 1981. Sediment accumulation rates and the completeness of stratigraphic sections. *Journal of Geology* 89 (5), 569–584.
- Sommerfield, C.K., Nittrouer, C.A., 1999. Modern accumulation rates and a sediment budget for the Eel shelf: a flood-dominated depositional environment. *Marine Geology* 154, 227–241.
- Wheatcroft, R.A., Borgeld, J.C., 2000. Oceanic flood deposits on the northern California shelf: large-scale distribution and small-scale physical properties. *Continental Shelf Research* 20, 2163–2190.
- Wheatcroft, R.A., Sommerfield, C.K., Drake, D.E., Borgeld, J.C., Nittrouer, C.A., 1997. Rapid and widespread dispersal of flood sediment on the Northern California Margin. *Geology* 25 (2), 163–166.
- Wilmshurst, J.M., 1997. The impact of human settlement on vegetation and soil stability in Hawke's Bay New Zealand. *New Zealand Journal of Botany* 35, 97–111.
- Wilmshurst, J.M., Eden, D.N., Froggatt, P.C., 1999. Late Holocene forest disturbance in Gisborne, New Zealand: a comparison of terrestrial and marine pollen records. *New Zealand Journal of Botany* 37, 523–540.
- Wilmshurst, J.M., McGlone, M.S., Partridge, T.R., 1997. A late Holocene history of natural disturbance in lowland podocarp/hardwood forest, Hawke's Bay, New Zealand. *New Zealand Journal of Botany* 35, 79–96.
- Wood, M.P., 2006. Sedimentation on a high input continental shelf at the active Hikurangi Margin: Poverty Bay, New Zealand. Master's thesis: School of Geography, Environment and Earth Sciences, Victoria University of Wellington.